JOC The Journal of Organic Chemistry

Article

pubs.acs.org/joc

Quaterpyridine Ligands for Panchromatic Ru(II) Dye Sensitizers

Carmine Coluccini,[†,‡] Norberto Manfredi,[†] Matteo M. Salamone,[†] Riccardo Ruffo,[†] Maria Grazia Lobello,[‡] Filippo De Angelis,*[,‡] and Alessandro Abbotto*[,†]

[†]Department of Materials Science and Milano-Bicocca Solar Energy Research Center - MIB-Solar, University of Milano-Bicocca, Via Cozzi 53, I-20125, Milano, Italy

[‡]Computational Laboratory for Hybrid/Organic Photovoltaics (CLHYO), Istituto CNR di Scienze e Tecnologie Molecolari, Via Elce di Sotto 8, 06123 Perugia, Italy

Supporting Information

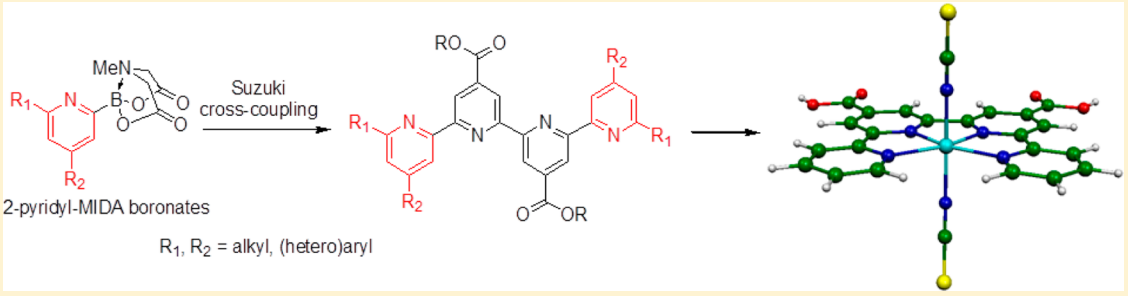

ABSTRACT: A new general synthetic access to carboxylated quaterpyridines (qpy), of interest as ligands for panchromatic dye-sensitized solar cell organometallic sensitizers, is presented. The strategic step is a Suzuki−Miyaura cross-coupling reaction, which has allowed the preparation of a number of representative unsubstituted and alkyl and (hetero)aromatic substituted qpys. To bypass the poor inherent stability of 2-pyridylboronic acid derivatives, we successfully applied *N*-methyliminodiacetic acid (MIDA) boronates as key reagents, obtaining the qpy ligands in good yields up to (quasi)gram quantities. The structural, spectroscopic (NMR and UV−vis), electrochemical, and electronic characteristics of the qpy have been experimentally and computationally (DFT) investigated. The easy access to the bis-thiocyanato Ru(II) complex of the parent species of the qpy series, through an efficient route which bypasses the use of Sephadex column chromatography, is shown. The bis-thiocyanato Ru(II) complex has been spectroscopically (NMR and UV−vis), electrochemically, and computationally investigated, relating its properties to those of previously reported Ru(II)−qpy complexes.

INTRODUCTION

Polypyridine ligands are extensively used in materials for a variety of scientific and technological applications, including nonlinear optics (NLO),[1,2] photovoltaics (PV),[3] and light emission.[4] In the field of molecular-based photovoltaic devices, dye-sensitized solar cells (DSCs)[5] presently hold the best promise for an optimal efficiency-cost trade-off, bypassing one of the most severe limitations of conventional PV systems such as silicon solar panels.[6,7] In a DSC device, the first chemical interface to the external solar input, thus representing one of the strategic components of the cell, is the photosensitizer dye. This molecule, after being promoted to an excited state upon sunlight absorption, transfers an electron to the TiO_2 semiconductor and a hole to a redox mediator. Electrons and holes are then collected to the cell anode and cathode, respectively. 2,2′-Bipyridine (bpy)-based Ru(II) complexes have been by far the most investigated and efficient systems, with efficiencies topping out at ca. 11% under standard AM 1.5 conditions for the benchmark dye bis(bpy-4,4′-dicarboxylate)-ruthenium(II) (N719).[8] One of the major issues for further improvement in the DSCs is the mismatch between the dye absorption spectrum and the solar emission, which extends to the near-IR (NIR) region. The design of new sensitizers having a strong panchromatic vis−NIR response is therefore of paramount importance for improving the cell light harvesting and, accordingly, its energy conversion efficiency.

One of the most successful strategies to optimize the optical properties of bpy-based Ru(II) complexes involves the insertion of π-electron donor (hetero)aromatic substituents in the π-conjugated backbone of the bpy ligand.[9] In particular, the use of alkoxy-substituted benzene rings and electron-rich thiophene-based moieties strongly improves the optical absorption of the sensitizers in terms of bathochromic and hyperchromic effects. These favorable properties in turn yielded DSCs with superior light harvesting abilities, higher external quantum efficiencies (ratio of produced electrons over incident photons), improved device photocurrents, and top-ranked power conversion efficiencies reaching almost 12%.[9] We have previously described the design and DSC application of a number of five-membered heteroaromatic substituted bpy[10] and phenyl-

Received: June 13, 2012
Published: August 23, 2012

   dx.doi.org/10.1021/jo301226z | J. Org. Chem. 2012, 77, 7945−7956

Scheme 1. General Synthetic Route to qpy Derivatives via Stille Cross-Coupling Reaction

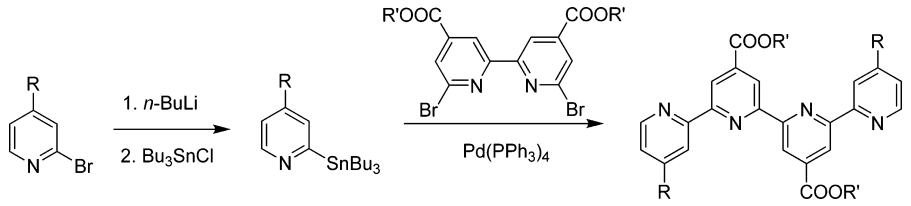

pyridine[11] ligands for coordination compounds and cyclometalated complexes.

Compared to the vast investigation on bpy-based DSC dyes, other ligands containing three or four conjugated pyridine rings in the 2,2′-positions have been scantly reported. This was mainly due to the more difficult synthetic access, considering that the insertion of more than two azine rings in the polypyridine ligand provides only beneficial effects. Indeed, the commonly known black dye, which is one of the very few sensitizers for which an efficiency larger than 11% has been reported, is a carboxylated terpyridyl complex of tris-thiocyanato Ru(II).[12] Such large efficiency is due to the fact that the black dye, when anchored to TiO_2, absorbs over the whole vis range extending into the NIR region up to 920 nm. The obvious improvement of such design is the extension to quaterpyridines (qpy) ligands for DSC complexes. Indeed, previous reports have pointed out the remarkable panchromatic response of qpy complexes spanning from the NIR to the UV spectral region, rendering them as alternative promising sensitizers with enhanced solar harvesting capability over the conventional bpy-based sensitizers.[13]

Metal complexes based on qpy ligands have been less commonly investigated mainly because of the more difficult synthetic access. Apart from the few DSC investigations,[13,14] the coordination behavior of qpy ligands has been systematically investigated for the first time by Constable and coworkers,[15] followed by other complexation studies.[16] The general route to carboxylated qpy, which contains the carboxylic groups needed for anchoring the dye to the TiO_2 nanoparticles, has been based on a convergent-like Stille cross-coupling reaction of 6,6′-dibromo-4,4′-alkoxycarbonyl-2,2′-bipyridine with 2-stannylpyridine derivatives, available through stannylation of the corresponding 2-bromopyridine precursor (Scheme 1).[13] However, this reaction suffers from a few limitations, such as use of toxic organotin compounds, limited yields, low reproducibility, and need of harsh conditions, thus hampering a systematic broad investigation or a successful market development. We have recently reported the first example of a heteroarylvinylene π-conjugated quaterpyridine Ru(II) sensitizer (N1044).[14] Indeed, this dye presented an effective panchromatic absorption band, covering the entire vis spectrum up to the NIR region, and optimal HOMO/LUMO and bandgap energies compared to previous Ru(II) qpy sensitizers. In particular, a record incident-photon-to-current efficiency (IPCE) from 360 to 920 nm was measured with a maximum of 65% at 646 nm and still 33% efficiency at 800 nm, that is, a spectral region where the efficiency of the prototype bpy Ru(II) dye N719, as well as that of the vast majority of the organometallic and organic DSC dyes, drops to zero. The high IPCE response in turn afforded a remarkably high cell photocurrent (19.2 mA cm^{-2}). Again, a Stille cross-coupling reaction was used starting from 4-[2-(3,4-ethylenedioxythien-2-yl)vinyl]-2-(trimethylstannyl)pyridine.

It is evident that such synthetic issues have so far impeded a systematic investigation of qpy-Ru(II) DSC sensitizers in spite of their very promising properties. It is therefore essential to develop new synthetic routes to carboxylated qpy, which should possibly be the most general as possible, high-yielding, easily up-scalable, and sustainable. In this way, a large variety of qpy complexes can be obtained and an industrial application becomes viable.

In this work, we describe a general synthetic access to carboxylated quaterpyridine ligands, of interest for DSC Ru(II) sensitizers, via the Suzuki–Miyaura cross-coupling reaction. This reaction takes advantage of the higher accessibility and stability, ease of handling and preparation, and low toxicity of boronic acid derivatives,[17] rendering this approach particularly useful for a systematic screening and full-scale production. The herein described synthetic scheme presents good yields and general applicability, easily extendible to other interesting examples pertaining to this class, including the possibility of preparing gram quantities of carboxylated qpy. In particular, we describe the synthesis and the experimental and computational investigation of the photophysical and electrochemical properties of a number of representative unsubstituted and π-donor conjugated 2,2′:6′,2″:6″,2‴-qpys with 2 carboxylic functionalities on the 4′,4″ central pyridines positions, thus providing the required chemical anchoring to the TiO_2 film used in DSC devices (Chart 1). In order to demonstrate the potential of these ligands to the synthesis of complexes, we also describe the preparation of the corresponding bis-thiocyanato Ru(II) complex with the simplest qpy ligand of the series. The complex has been prepared through an efficient route which bypasses the use of time- and product-consuming Sephadex column chromatography, as commonly done for most DSC Ru(II) dyes.

Chart 1. General Structure of 4′,4″-Dicarboxylic-2,2′:6′,2″:6″,2‴-qpys Prepared in This Work

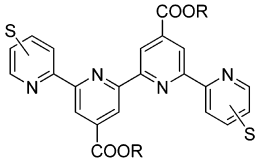

R = H, alkyl

S = H, aliphatic or (hetero)aromatic substituent

RESULTS AND DISCUSSION

Structure and Synthesis. The investigated qpy ligands, as diisobutyl esters, **1a**–**5a** are listed in Chart 2. The selected qpy identify a representative list of derivatives according to commonly known substituent effects or literature data on important DSC sensitizers. Ligand **1a** has no substitution on the pyridine rings, with the exception of the two central carboxylated groups. This ligand will be chosen as a reference system and will be used for the preparation of the

dx.doi.org/10.1021/jo301226z | J. Org. Chem. 2012, 77, 7945–7956

Chart 2. Substituted 4′,4″-Dicarboxylic-2,2′:6′,2″:6″,2‴-qpy Ligands Investigated in This Work

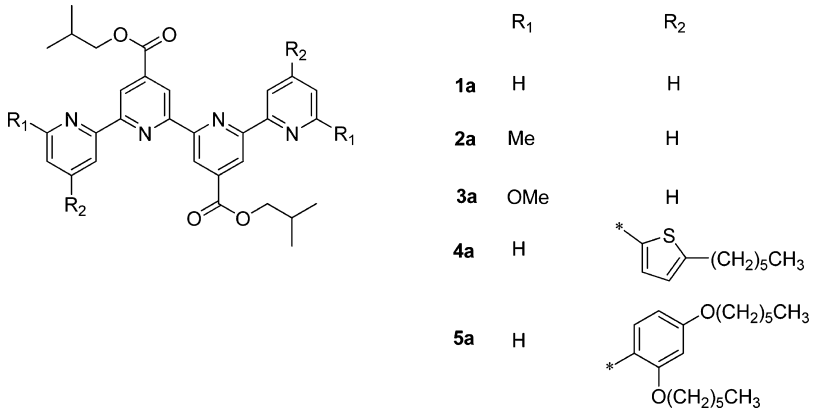

corresponding bis-thiocyanato Ru(II) complex. Ligands **2a** and **3a** present primary weak (alkyl) and strong donor (alkoxy) substituents, respectively. The remaining two examples carry (hetero)aromatic substituents on the peripheral rings. The thiophene substituents of ligand **4a** have been introduced because of the large amount of literature on efficient thiophene-based Ru(II) bpy DSC sensitizers, endowed with record efficiencies (see above).[9] Finally, ligand **5a** presents two *o,p*-dialkoxyphenyl substituents. This substituent has been recently embedded in highly performing DSC dyes (organic dye Y123)[18] that afforded the present record photovoltage of over 1 V[19] and, in cosensitized devices, an energy conversion efficiency of over 13%.[20]

The key synthetic step for the access to qpy **1a−5a** is represented by the final Pd-catalyzed Suzuki cross-coupling reaction by using the proper *N*-methyliminodiacetic acid (MIDA) boronates **1b−5b**. Despite the large potential of the Suzuki reaction, 2-pyridylboronic acids or their conventional (e.g., pinacol) esters are inherently unstable. This issue has so far strongly limited the application of the Suzuki cross-coupling reaction to 2-pyridyl derivatives. In contrast, Burke et al. have reported that 2-heteroarylboronic acid MIDA esters are benchtop air-stable reagents isolable in a chemically pure form and can be hydrolyzed in situ with weak bases slowly affording the corresponding unstable boronic acids, which promptly undergo a versatile coupling reaction with aryl and heteroaryl halides and sulfonates.[21] Recently, the wide applicability and general conditions for this reaction have been demonstrated.[22] We have now successfully applied this approach for the first time to the synthesis of qpy **1a−5a** by using the Pd-catalyzed cross-coupling reaction between 2 equiv of substituted 2-pyridyl-MIDA boronates **1b−5b** and di-isobutyl-6,6′-dichloro-2,2′-bipyridine-4′,4′-dicarboxylate (**6**) (Scheme 2). The diisobutyldichloro bpy derivative has been prepared applying a previously reported procedure for the synthesis of the corresponding bis(methyl ester).[13c]

A number of simple 2-pyridyl-MIDA boronates are now available from commercial suppliers. Among those, we have selected **1b−3b** for the above-described reasons. When not available, as in the case of the more elaborate derivatives **4b** and **5b**, the MIDA boronates were conveniently prepared according to a procedure reported in the literature starting from the bromo precursors **4c** and **5c** via the transligation of 2-pyridyl trialkoxyborate salts with MIDA (Scheme 3).[23] The bromo derivatives **4c** and **5c** were either previously reported by us or synthesized according to the described procedure involving a

Scheme 2. Synthesis of qpy 1a−5a via Suzuki Cross-Coupling Reaction of 2-MIDA Pyridines 1b−5b (R_1 and R_2, Chart 2)

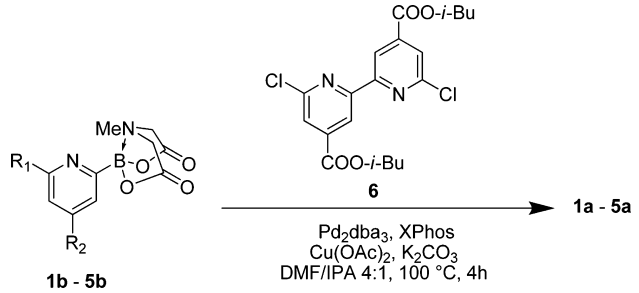

Scheme 3. Synthesis of 2-Pyridyl MIDA Boronate 4b and 5b (R_2 as in Chart 2)

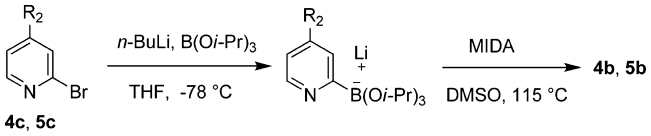

regioselective Suzuki cross-coupling reaction of 2-bromo-4-iodopyridine.[24]

The yields of the Suzuki cross-coupling reaction of 2-MIDA-pyridines **1b−5b** to qpy **1a−5a** are collected in Table 1. The

Table 1. Yields of the Suzuki Cross-Coupling Reactions from MIDA Boronates to Quaterpyridine 1a - 5a

qpy	MIDA boronate	yield (%)
1a	**1b**	33
2a	**2b**	21
3a	**3b**	34
4a	**4b**	38
5a	**5b**	39

yields were always higher than 20%, and reference ligand **1a** was prepared on gram scale. These data, along with the fact that the MIDA boronate precursors and the other reactants and catalysts are either commercially available or readily synthesized, suggest the wide applicability of the described procedure to the unprecedented fast and convenient synthesis of substituted quaterpyridines.

To check the applicability of the synthesized qpy ligands to the preparation of ruthenium DSC sensitizers, we have

dx.doi.org/10.1021/jo301226z | J. Org. Chem. 2012, 77, 7945−7956

Scheme 4. Synthesis of qpy-Based Ru(II) Complex 1d

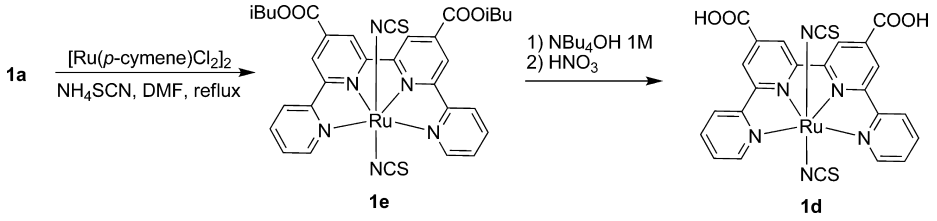

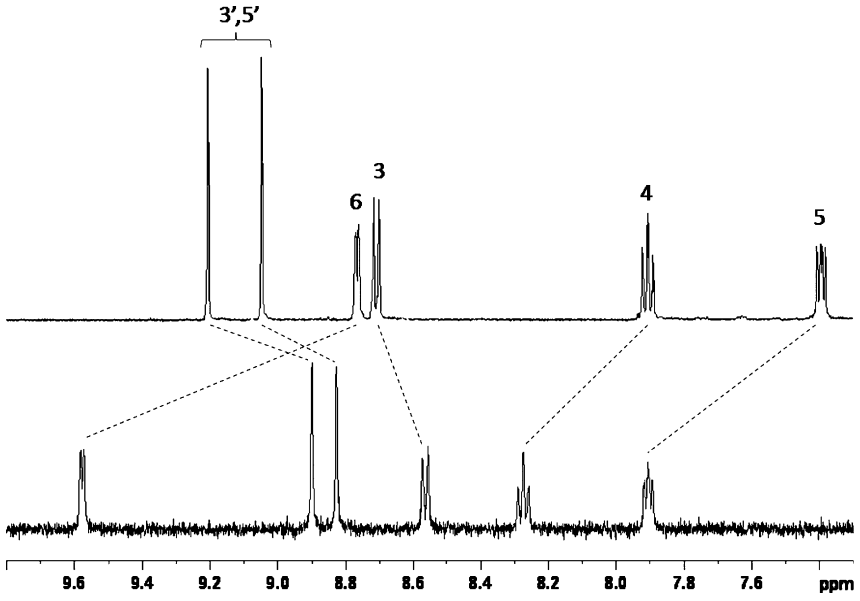

Figure 1. ^{1}H NMR spectra of the qpy ligand **1a** (in $CDCl_3$) and its Ru(II) complex **1d** (in MeOD) (aromatic region).

synthesized, as a preliminary test, the bis-thiocyanato Ru(II) complex **1d** containing the most simple qpy ligand **1a**. By doing this, we have decided to develop a new procedure which bypasses the use of tedious and time-consuming repeated Sephadex LH-20 gravimetric column chromatography, as routinely done for the synthesis of the benchmark DSC dye N7198 and other Ru(II) bpy dyes as well as for previously described qpy-complexes.[13,14] The protection of the carboxylic functionalities with isobutyl ester groups and purification avoiding the Sephadex gravimetric chromatography has been described for N719.[25] In our case, purification is easily performed by a single flash chromatography on silica gel of the bis-ester precursor complex **1e**, easily prepared from the bis-ester ligand **1a** by reaction with dichloro(*p*-cymene)-ruthenium(II) dimer, as shown in Scheme 4. Mild hydrolysis of the isobutyl ester functionalities and titration with HNO_3 afforded the bis-carboxylic Ru(II) complex **1d** in good yields.

Spectroscopic Characterization of Ligands 1a−5a and Complex 1d. The ligands **1a−5a** and the complex **1d** have been characterized by ^{1}H NMR spectroscopy. The ^{1}H NMR spectrum of the complex **1d**, along with that of the corresponding qpy ligand **1a**, is shown in Figure 1. Because of solubility requirements of the former compound, spectra are compared in different solvents. To allow direct comparison with literature data, the same solvents reported for similar ligands and complexes were selected.[13] However, in principle, some of the conclusions of the subsequent comparative discussion could be partially revised considering potential significant solvent effects on the chemical shifts. Both spectra are in agreement with those of previous qpy ligands and complexes reported in the literature.[13,14] It should be noted, however, that the absence of substituents in the ring 4,4‴ sites of the terminal pyridines allowed an unequivocal assignment of the heteroaromatic protons thanks to the modified splitting patterns, preventing previously reported misassignments.[13] The most evident patterns are the two singlets at ca. 9.2 and 9.0 ppm in the ligand, clearly assigned to the positions 3′ and 5′ of the median pyridine rings, which are high-field shifted to ca. 8.9 and 8.8 ppm in the complex. In contrast, the positions pertaining to the terminal heteroaromatic rings are on average significantly downfield shifted from **1a** to **1d**. In particular, H-6 (doublet) is low-field shifted from 8.8 to 9.6 ppm, and though to a lower extent, H-4 (triplet) and H-5 (dd) are shifted by ca. +0.5 ppm. The proton in position 3 (doublet) is almost unvaried. In summary, apart from possible solvent effects, the two terminal and the two central pyridine rings are low-field and high-field shifted, respectively, as a consequence of the metal ion coordination, in contrast to previous findings.[13]

The electronic absorption spectra of qpy **1a−5a** are shown in Figure 2. Table 2 collects the main optical parameters in CH_2Cl_2. All of the ligands presented two main bands in the 250−350 nm region and a low absorption sideband around 400 nm. To rule out the hypothesis that this low energy band could be associated with the presence of pyridinium moieties arising from protonation of the pyridine groups by solvent acidic impurities, spectra were checked in the presence of an excess of sodium hydroxide, confirming that the line shape did not differ from that in absence of base. The high-energy UV band is always more intense, with the exception of **4a**. The intensity of the absorption importantly increases on going from **1a** to **5a**, as

dx.doi.org/10.1021/jo301226z | J. Org. Chem. 2012, 77, 7945−7956

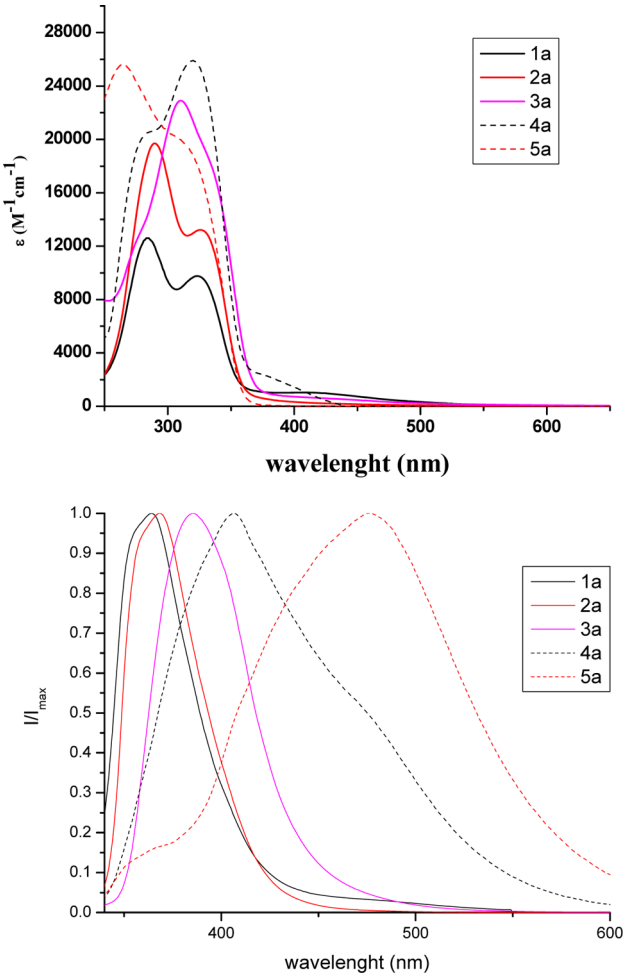

Figure 2. Absorption (top) and normalized emission (bottom) spectra of quaterpyridines **1a**–**5a** in CH_2Cl_2.

Table 2. Experimental and Computed Optical Absorption Data of Quaterpyridines 1a–5a[a] and Ru(II) Complex 1d[b]

compd	λ_{abs} (λ_{calc}) (nm)	ε (M^{-1} cm^{-1})	λ_{em} (nm)	E_{gap}[c] (eV)	E_{0-0}[d] (eV)
1a	284 (263)[e]	12600 ± 300	364	3.6	3.6
	323 (302)[e]	10000 ± 300			
2a	291 (267)[e]	19700 ± 200	368	3.5	3.6
	327 (307)[e]	12700 ± 200			
3a	310 (304)[e]	22900 ± 200	386	3.5	3.5
4a	319 (301)[e]	25900 ± 400	407	3.5	3.5
5a	264 (270)[e]	25600 ± 600	476	3.5	3.5
1d	345 (305)[f]	15900 ± 100		1.7	
	525 (540)[f]	4500 ± 100			
	630 (723)[f]	5100 ± 100			
1d[g]	342 (316)[f]			1.8	
	358				
	521 (502)[f]				
	614 (607)[f]				

[a]In CH_2Cl_2. [b]In DMF. [c]Optical band gaps estimated using the method of Tauc plot. [d]Zero–zero transition energy estimated from the intercept of the normalized absorption and emission spectra. [e]Calculated using the MPW1K functional. [f]Calculated using the B3LYP functional. [g]Deprotonated complex (experimental spectra were measured in the presence of NaOH).

a clear consequence of the hyperchromic effect induced by the aliphatic and (hetero)aromatic π-donor substituents. In particular, the most significant increment compared to the pristine ligand **1a** is recorded for the thiophene-substituted **4a** and the dihexyloxyphenyl-substituted **5a** qpy, with a maximum molar extinction coefficient ε increasing from ca. 10000 in **1a** to over 25000 M^{-1} cm^{-1} in **4a** and **5a**. The high-energy band, located at 250–350 nm, is attributed, on the basis of the computational investigation, to $\pi-\pi^*$ transitions mainly involving the central pyridine units. This result is notable in view of the integration of the ligand in panchromatic DSC Ru(II) complexes, where a more intense light harvesting is essential for improved cell photocurrents and energy conversion efficiencies. The onset values and optical band gaps listed in Table 2 were estimated using the Tauc plots (Supporting Information).[26] The Tauc plot is used to determine the optical gap of molecules and thin film materials by plotting the quantity $(\alpha h\nu)^2$, where α is the absorption coefficient (cm^{-1}), vs the energy of the absorbed photon $h\nu$. The value of the optical band gap is obtained by extrapolating the linear behavior to the abscissa. The investigated qpy showed variable emission properties with an emission peak shifting from 364 nm for **1a** to 476 nm for **5a** (Figure 2). Excitation spectra of the qpy ligands showed peaks at identical or similar positions of their absorption peaks, though the relative intensity of the bands is different (see the Supporting Information). Therefore, in particular for **3a**–**5a**, the presence of emissive aggregates cannot be excluded.

In Figure 3 we compared the experimental and computed UV–vis spectra of complex **1d** (deprotonated species, see the Supporting Information for the protonated species and solvatochromism). Figure 3 clearly shows evidence of the panchromatic absorption character spanning from the UV to the NIR region of the spectrum. The spectrum well matches those of previously reported qpy-based Ru(II) complexes with alkyl substituents on the terminal pyridine rings.[13c] In particular, the vis portion of the spectrum of deprotonated **1d** is dominated by two bands at 614 and 521 nm and a sideband at ca. 460 nm. Both computed bands at 607 and 502 nm are blue-shifted by only 0.04 and 0.09 eV, respectively, compared to experimental spectrum. The computed bands have the same intensity of the experimental band. A shoulder at 462 nm was also computed. Both bands are assigned to metal-to-ligand charge-transfer (MLCT) transitions, which are typical of these complexes, while the intense absorption in the UV region is attributed to intraligand $\pi-\pi^*$ transitions. The absorption broadness, comparable to that of the very efficient black dye (tris-thiocyanato-Ru(II) terpyridyl),[27] clearly originates from the extended π-conjugation of the qpy ligand compared to the more common bpy complexes. No important experimental and computed solvatochromism of the deprotonated **1d** was found (see the Supporting Information), suggesting that the dielectric does not influence the absorption spectra. The complex **1d** did not show significant emission intensities.

Attenuated Total Reflection Fourier Transform IR (ATR-FTIR) spectrum of the complex **1d** was measured as a solid sample (Figure 4). The most relevant feature is the intense band centered at 2097 cm^{-1}, which is assigned to the CN stretching of the thiocyanate groups. The presence of a single band at this energy value suggests that the two ancillary ligands are coordinated to the metal center through the nitrogen atom in a *trans* configuration.[13,14,28] The second most important signal, at 1728 cm^{-1}, is due to the ν(C═O) of the carboxylic

dx.doi.org/10.1021/jo301226z | J. Org. Chem. 2012, 77, 7945–7956

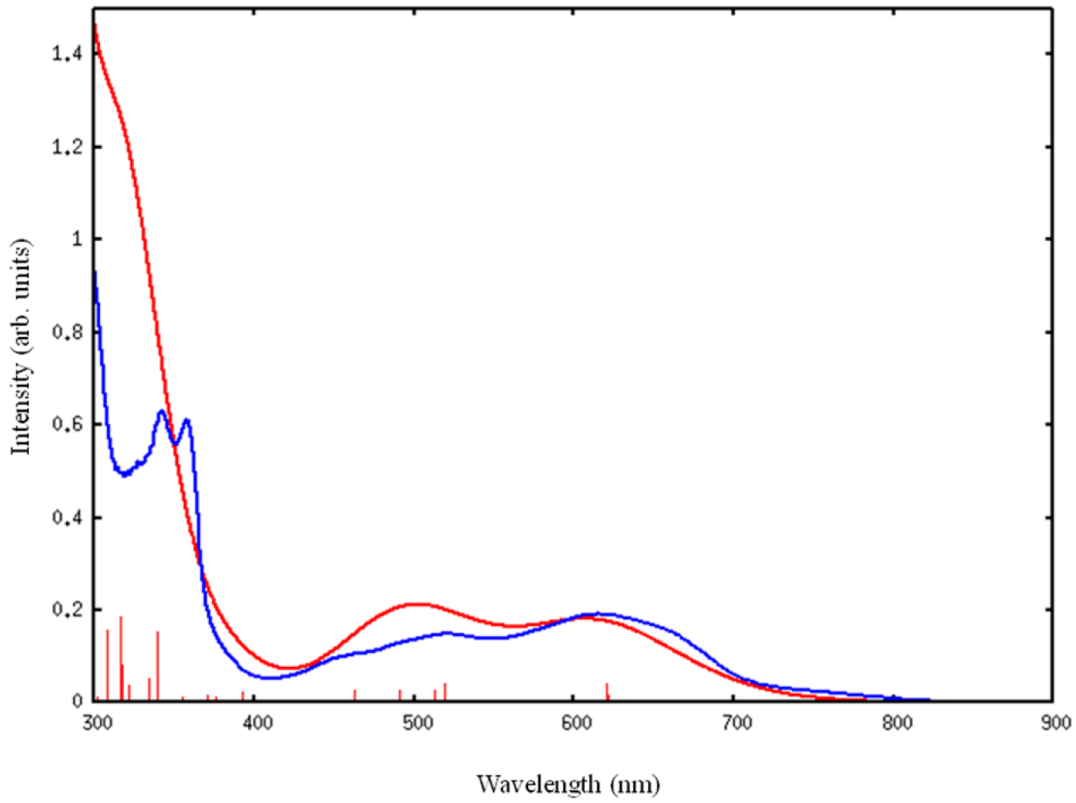

Figure 3. Comparison between computed (red line) and experimental (blue line) UV−vis spectra of deprotonated complex **1d** (DMF). Red vertical lines correspond to the calculate excitation energies and oscillator strengths.

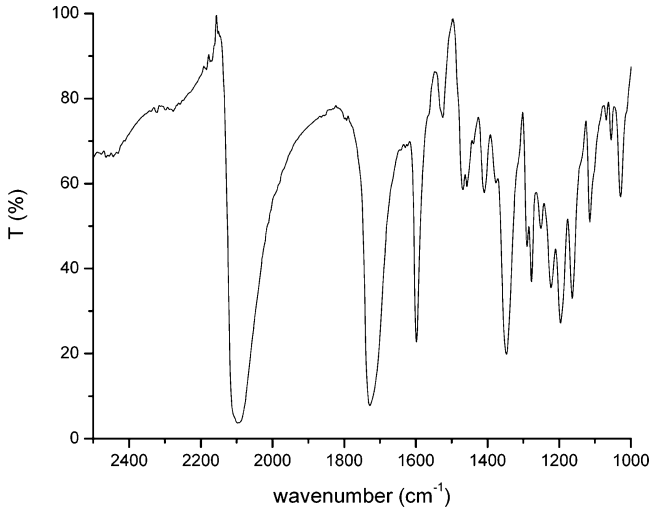

Figure 4. ATR−FTIR spectrum of complex **1d** (powder).

groups. Finally, the intense band at 1598 cm^{-1} is associated to the ring stretching modes of the azine rings.[13,14]

Electrochemical Characterization. The electrochemical properties of qpy **1a**−**5a** were examined by cyclic voltammetry (CV) in dichloromethane (CH_2Cl_2). Current potential profiles are shown in Figure S4 (Supporting Information). The redox processes related to the molecule reduction (potential <−1.5 V vs Fc^+/Fc reference couple) showed an irreversible character. The oxidation potentials were expected to be high (deep HOMO energies) due to the presence of the four strong electron-withdrawing pyridine moieties in the molecules, though the presence of electron-donating alkyl and aromatic substituents should have the effect of lowering the potential (see the aforementioned computational investigation). Indeed, the oxidation processes were not detectable since they matched the high voltage limit of the electrolyte ($TBAClO_4$ in CH_2Cl_2) decomposition. For this reason, only LUMO values could be measured by electrochemistry. Due to the difficulty in defining the reductive current onsets, we preferred to apply differential pulsed voltammetry (DPV) for the estimation of the LUMO energy levels (Figure 5). The reduction peaks are located in a narrow potential range (from −2.07 to −2.16 V vs Fc^+/Fc), thus leading to similar calculated LUMO energy levels as

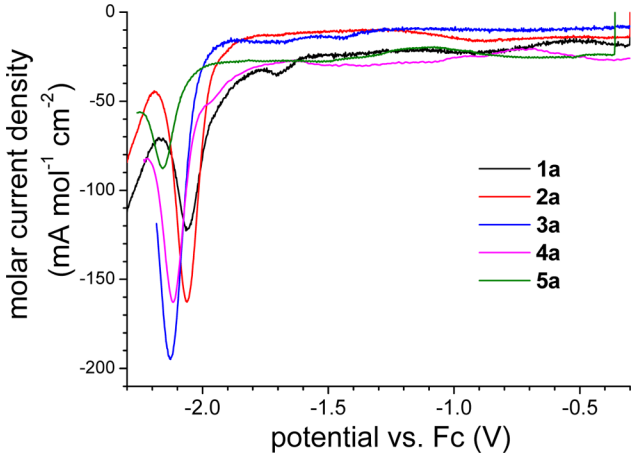

Figure 5. DPV current/potential profiles of qpy **1a**−**5a** in 0.1 M $TBAClO_4/CH_2Cl_2$ electrolyte (20 mV/s).

dx.doi.org/10.1021/jo301226z | J. Org. Chem. 2012, 77, 7945−7956

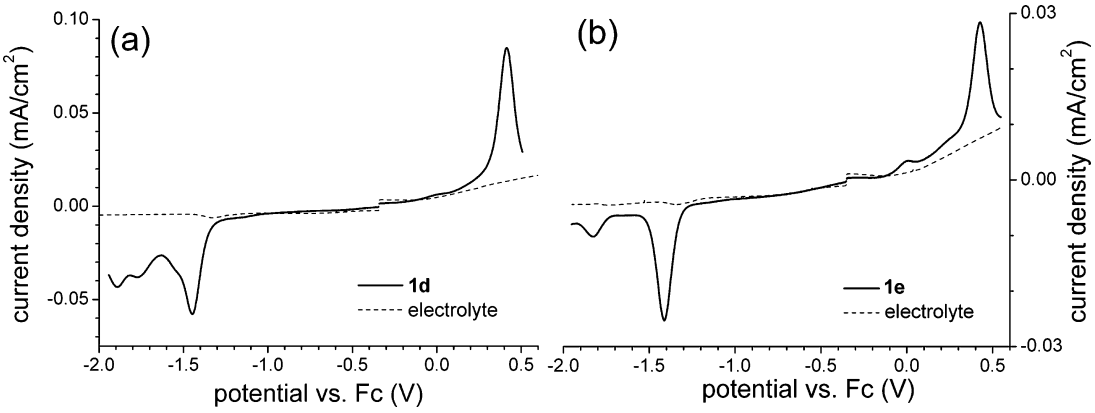

Figure 6. DPV current/potential profiles of (a) complex **1d** and (b) complex **1e** (on glassy carbon working electrode).

actually confirmed by the computational investigation (vide infra).

The CV current/potential profiles of complexes **1d** and **1e** in DMF showed irreversible features of the current waves (Figure S5, Supporting Information). Thus, the redox electrochemical potentials were obtained from the current onsets of the DPV traces (Figure 6). The oxidation of the two complexes is a metal-centered process at high voltages (0.34 V vs Fc^+/Fc). Therefore, the oxidation process is independent of the carboxylic functionalization. The oxidation potential, related to the Ru(II)/Ru(III) equilibrium, is similar to that previously reported for other qpy Ru(II).[13,14] On the reduction side, a first negative potential was measured at −1.35 V vs Fc^+/Fc (current onset) for the **1d** complex (see Figure 6a). This reduction step was previously associated to the protons of the carboxylic acid functionalities.[13,14,29] A second reduction step, which occurred at more negative potentials (−1.87 V vs Fc^+/Fc), was attributed in previous works to the reduction of the qpy ligand[13,14] and matches that reported for the reduction of the 4,4‴-di-*tert*-butyl-qpy corresponding derivative (−1.93 V).[13c] In order to properly assign the two reduction steps and discriminate between the reduction of the carboxylic protons and the ligand, we have also investigated the reduction behavior of the diester precursor **1e**. In this case, a first reversible reduction was observed at −1.32 V vs Fc^+/Fc, which is very close to that found for the bis-COOH derivative **1d**. Since for **1e** the first reduction process necessarily involves the qpy ligand, as the carboxylic protons are absent, this finding suggests that the first reduction step might be related to the reduction of the ligand as well. UV−vis spectroelectrochemistry experiments for the complex **1d** confirmed that both reduction processes were associated to a change in the MLCT absorption bands (Figure S6, Supporting Information).[30] The electrochemical results are summarized in Table 3. It should be noted that, by using the described interpretation, the electrochemical band gap of **1d** and **1e** (ca. 2 eV) nicely matches the optical band gap. If the reduction of the ligand in **1d** would have been associated to the second reduction step as previously reported,[13,14] a higher electrochemical band gap of 2.3 V (that is, equal to that reported for the 4,4‴-di-*tert*-butyl qpy corresponding derivative)[13c] would have been determined, less properly fitting the optical data.

Computational Analysis. To gain insight into the structural, electronic, and optical properties of the investigated qpy ligand, we performed density functional theory (DFT) and time-dependent DFT (TDDFT) calculations. We simulated the absorption spectra of **1a**−**5a** in the 250−650 nm spectral range. We tested two different exchange-correlation functionals, B3LYP (Table S2, Supporting Information) and MPW1K, with two different percentages of Hartree−Fock exchange, 20 and 42, respectively. In general, we noted that for this type of organic systems the MPW1K results were in better agreement with experimental data compared to B3LYP results, as previous reported by Pastore et al. (see Table 2).[32]

Table 3. Electrochemical Data of Quaterpyridines 1a−5a[a] and Ru(II) Complexes 1d and 1e.[b]

compd	E_{red}[a] (V vs NHE)	E_{ox}[a] (V vs NHE)	LUMO[b] (eV)	HOMO[b] (eV)	E_{gap}[c] (eV)
1a[d]	−1.48		−3.1	−6.7[e]	
2a[d]	−1.47		−3.1	−6.7[e]	
3a[d]	−1.54		−3.1	−6.6[e]	
4a[d]	−1.53		−3.1	−6.6[e]	
5a[d]	−1.57		−3.0	−6.5[e]	
1d[f]	−0.72	0.97	−3.9	−5.6	1.7
1e[f]	−0.69	0.97	−3.9	−5.6	1.7

[a]The potentials measured vs Fc^+/Fc were converted into normal hydrogen electrode (NHE) potentials by addition of +0.59 and +0.63 V for CH_2Cl_2 and DMF, respectively. [b]Energy levels have been calculated by using a value of −4.6 eV vs vacuum for NHE (ref 31). [c]Electrochemical band gaps (HOMO−LUMO energy difference). [d]In CH_2Cl_2. [e]Estimated from measured LUMO energy and zero−zero transition energy from optical data (Table 2). [f]In DMF.

The isodensity plots of FMO are shown in Figure 7. From the energies of the frontier molecular orbitals (FMO) (Supporting Information) we notice that the LUMO energies are substantially less negative respect to the experimental values (Table 3). This was somehow expected considering the larger relaxation energy of the anionic species. We note that the HOMO levels are destabilized going from **1a** to **5a**. This destabilization is due to the different localization of orbitals. Indeed, the HOMO is localized on the four pyridines for **1a**−**3a**, and this determined only a slight variation in the energy level. Instead, for **4a** and **5a**, HOMO is localized on the thiophene and the dihexyloxyphenyl substituent, respectively, and the energy is 0.46 and 0.7 eV higher with respect to **1a**. For all of the investigated molecules, the LUMO is localized on the central pyridines carrying the carboxylic functionalities, and then it has about the same energy for all compounds. In agreement with the measured LUMO values, a slight LUMO destabilization is found going from **1a** to **5a** (Supporting Information). For the **1d** complex, the set of quasi-degenerate

dx.doi.org/10.1021/jo301226z | J. Org. Chem. 2012, 77, 7945−7956

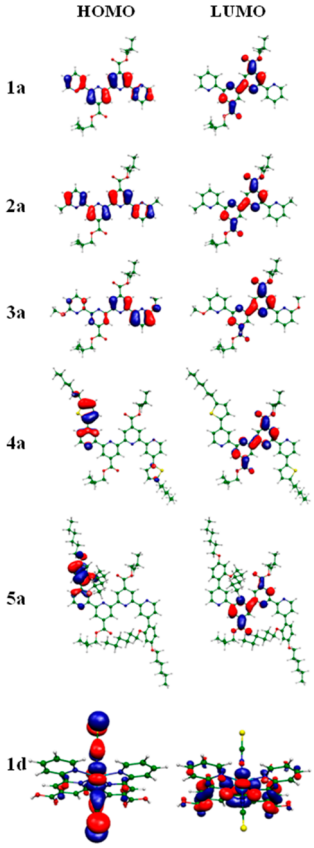

Figure 7. Isodensity surface plots (isodensity counter: 0.035) of **1a**–**5a** and **1d** HOMO and LUMO.

HOMO, HOMO-1, and HOMO-2 have essentially Ru t_{2g} character, while the LUMOs correspond to ligand π^* orbitals (Figure 7). The relevant e_g states are found as the LUMO+7/+8. The calculated HOMO value for **1d**, −5.55 eV, i.e., +0.95 V vs NHE, is in good agreement with the measured value. The LUMOs are in all cases slightly destabilized compared to experimental values; this can be somehow expected considering that these levels are calculated neglecting any relaxation upon reduction, which should induce larger differences than for the HOMOs.

CONCLUSIONS

Substituted quaterpyridines can play a crucial role in the fabrication of efficient dye-sensitized solar cells thanks to the unique panchromatic properties, ranging from UV–vis to NIR, of their metal complexes. Unfortunately, the difficult synthetic access (low yields, restricted quantities, low reproducibility) and the use of toxic organotin reagents of the so far reported Stille cross-coupling synthetic access has greatly limited this important potential. Here we have presented a new synthetic route to alkyl and (hetero)aryl substituted qpys that makes use of the more sustainable and up-scalable Suzuki cross-coupling reaction. The limited stability and applicability of 2-pyridylboronic acid and esters, which has impeded so far the application of the Suzuki coupling to the synthesis of polypyridines, has been bypassed by using stable 2-pyridyl MIDA derivatives, which were successfully coupled to a dichloro bpy intermediate readily affording a number of qpys in very satisfactory yields. Not only does this access make use of nontoxic boronic derivatives, but we have shown that the scope is general and can be systematically applied to the synthesis of variously substituted polypyridines. In the case of the parent compound of the series (**1a**), reactions producing quantities of nearly 1 g were performed, showing the scalability and the industrial potential of the proposed scheme. The new qpys were fully experimentally and computationally investigated in their structural, spectroscopic, electrochemical, and energetic properties. In particular, combined optical and electrochemical data have calculated HOMO values increasing from −6.7 eV in **1a** and **2a** to −6.5 eV in **5a**, as a consequence of the substitution with an electron-rich substituent. The estimated optical band gaps and zero–zero energies are very similar for all the ligands (3.5–3.6 eV).

The bis-thiocyanato Ru(II) complex **1d** of the parent qpy **1a** was prepared via a new route which avoids the use of tedious and time-consuming methods such as Sephadex column chromatography, routinely used in the synthesis of Ru(II) polypyridyl complexes. The NMR properties were compared to those of the ligand precursor showing that the terminal and central ring protons are low- and high-field shifted, respectively, in contrast with previous reports. Its panchromatic absorption features were confirmed. The electrochemical oxidation and reduction properties of the complex **1d**, and of its diester precursor **1e**, were investigated. The comparison of the two species suggested a different interpretation of the reduction process, in partial disagreement with previous reports.[13,14] For both complexes an electrochemical band gap of ca. 2 eV was measured.

In conclusion, we believe that the here presented synthetic scheme and multidisciplinary study of properties could represent an important step for the systematic investigation of qpy-based Ru(II) DSC dyes endowed with unusually efficient optical response and light harvesting properties and, ultimately, power conversion efficiencies.[33]

EXPERIMENTAL SECTION

Synthesis and Characterization. *General Methods.* NMR spectra were recorded on an instrument operating at 500.13 (^{1}H) and 125.77 MHz (^{13}C). ^{13}C multiplicities were assigned on the basis of the results of J-MOD experiments. HRMS measurements were performed using a ESI source and ion trap (Fourier transform ion cyclotron resonance FT-ICR) as a mass analyzer. Flash chromatography was performed with silica gel 230–400 mesh (60 Å). Reactions were performed in oven-dried glassware under nitrogen or in Schlenk flasks under argon, previously charged in a argon-filled glovebox. Reactions were monitored by thin-layer chromatography by using UV light (254 and 365 nm) as a visualizing agent. All reagents were obtained from commercial suppliers at the highest purity and used without further purification. Anhydrous solvents were purchased from commercial suppliers and used as received. Extracts were dried with Na_2SO_4 and filtered before removal of the solvent by evaporation.

*4-(5-Hexylthien-2-yl)-2-pyridinylboronic Acid MIDA Ester (**4b**).* Triisopropyl borate (0.5 mL, 2.9 mmol), **4c**[24] (470 mg, 1.45 mmol) and THF (10 mL) were added to a Schlenk flask under an argon atmosphere. The solution was cooled to −78 °C, and *n*-BuLi (1.5 mL, 1.6 M in hexane) was slowly added. The mixture was stirred for 1 h at −78 °C and for 3 h at room temperature. Separately, a three-necked flask, equipped with a thermometer, a water-cooled distillation apparatus, and an addition funnel, was charged with MIDA (362 mg, 2.5 mmol) and dry DMSO (5 mL) under inert atmosphere and the mixture heated at 120 °C. The previously prepared borate solution was charged in the addition funnel and added dropwise to the hot and stirred solution of MIDA in DMSO, maintaining the temperature at 100 °C. During the addition, THF was simultaneously distilled off. The reaction mixture was cooled to 70 °C and DMSO distilled off under vacuum. The mixture was then adsorbed onto Celite with

dx.doi.org/10.1021/jo301226z | J. Org. Chem. 2012, 77, 7945–7956

CH_3CN (1 mL). CH_3CN was evaporated under vacuum, and the Celite powder was subjected to flash chromatography (ethyl acetate/CH_3CN 1:1). The product was obtained as a transparent oil (160 mg, 0.40 mmol, 28%) that was submitted in the subsequent step without further purification (MIDA is present as a residual impurity; see ^1H and ^{13}C NMR spectra in the Supporting Information). ^1H NMR (DMSO-d_6): δ 8.64 (d, J = 5.2 Hz, 1H), 7.67 (d, J = 1.3 Hz, 1H), 7.63 (d, J = 3.6 Hz, 1H), 7.54 (dd, J = 2.0, 5.1 Hz, 1H), 6.94 (d, J = 3.6 Hz, 2H), 4.40 (d, J = 17.0 Hz, 2H), 4.10 (d, J = 17.0 Hz, 2H), 2.84 (t, J = 7.5 Hz, 4H), 2.60 (s, 3H), 1.66 (quin, 7.5 Hz, 2H), 1.4−1.2 (m, 6H), 0.87 (t, J = 7.0 Hz, 3H). ^{13}C NMR (CD_3CN): δ 168.6 (C, 2C), 150.5 (CH, 1C), 148.5 (C, 1C), 140.2 (C, 1C), 138.6 (C, 1C), 126.0 (CH, 1C), 125.8 (CH, 1C), 122.7 (CH, 1C), 118.5 (CH, 1C), 62.1 (CH_2, 2C), 46.7 (CH_3, 1C), 31.3 (CH_2, 1C), 31.2 (CH_2, 1C), 29.8 (CH_2, 1C), 28.4 (CH_2, 1C), 22.3 (CH_2, 1C), 13.3 (CH_3, 1C). ESI-HRMS: calcd for $[M + H]^+$ $C_{20}H_{26}BN_2O_4S$ 401.1701, found 401.1695.

*2-Bromo-4-(2,4-dihexyloxyphenyl)pyridine (**5c**).* A mixture of 4,4,5,5-tetramethyl-2-(2,4-dihexyloxyphenyl)-1,3,2-dioxaborolane[18a] (499 mg, 1.23 mmol), 2-bromo-4-iodopyridine (349 mg, 1.23 mmol), $Pd(PPh_3)_4$ (71 mg, 0.061 mmol), and Na_2CO_3 (208 mg, 1.96 mmol) in THF (30 mL) and H_2O (20 mL) was stirred under microwave irradiation (100 W, 100 °C) for 30 min. THF was evaporated, and H_2O (20 mL) was added. The aqueous solution was extracted with CH_2Cl_2 (3 × 50 mL). The organic layers were dried with Na_2SO_4, and CH_2Cl_2 was evaporated. Flash chromatography (petroleum ether/CH_2Cl_2 95:5) afforded **5c** as a transparent oil (290 mg, 0.66 mmol, 54%). ^1H NMR ($CDCl_3$): δ 8.31 (d, J = 5.2 Hz, 1H), 7.70 (d, J = 1.0 Hz, 1H), 7.42 (dd, J = 1.5, 5.2 Hz, 1H), 7.26 (d, J = 8.4 Hz, 1H), 6.55 (dd, J = 2.3, 8.4 Hz, 1H), 6.52 (d, J = 2.3 Hz, 1H), 4.00−3.95 (m, 4H), 1.92−1.72 (m, 4H), 1.5−1.4 (m, 4H), 1.4−1.3 (m, 8H), 0.92 (t, J = 7.0 Hz, 3H), 0.90 (t, J = 7.0 Hz, 3H). ^{13}C NMR ($CDCl_3$): δ 161.5 (C, 1C), 157.4 (C, 1C), 149.3 (CH, 1C), 149.1 (C, 1C), 142.0 (C, 1C), 130.9 (CH, 1C), 128.0 (CH, 1C), 123.0 (CH, 1C), 118.6 (CH, 1C), 105.7 (CH, 1C), 100.2 (CH, 1C), 68.4 (CH_2, 1C), 68.2 (CH_2, 1C), 31.6 (CH_2, 1C), 31.5 (CH_2, 1C), 29.2 (CH_2, 1C), 29.0 (CH_2, 1C), 25.9 (CH_2, 1C), 25.7 (CH_2, 1C), 22.6 (CH_2, 1C), 22.6 (CH_2, 1C), 14.0 (CH_3, 1C), 14.0 (CH_3, 1C). ESI-HRMS: calcd for $[M + H]^+$ $C_{23}H_{33}{}^{79}BrNO_2$ 434.1689, found 434.1702; calcd for $[M + H]^+$ $C_{23}H_{33}{}^{81}BrNO_2$ 436.1669, found 436.1682.

*4-(2,4-Dihexyloxyphenyl)-2-pyridinylboronic Acid MIDA Ester (**5b**).* The same procedure for the synthesis of **4b** was applied using triisopropyl borate (0.12 mL, 0.70 mmol), **5c** (210 mg, 0.48 mmol), THF (5 mL), *n*-BuLi (0.45 mL, 1.6 M in hexane), MIDA (241 mg, 0.82 mmol), and dry DMSO (5 mL). The product was obtained as a transparent oil (91 mg, 0.18 mmol, 37%), which was submitted in the subsequent step without further purification. ^1H NMR (CD_3CN): δ 8.66 (dd, J = 0.5, 5.2 Hz, 1H), 7.83 (d, J = 1.0 Hz, 1H), 7.50 (dd, J = 1.9, 5.1 Hz, 1H), 7.38 (d, J = 9.1 Hz, 1H), 6.67−6.60 (m, 2H), 4.15 (d, J = 16.8 Hz, 2H), 4.08−4.02 (m, 4H), 3.83 (d, J = 16.8 Hz, 2H), 2.62 (s, 3H), 1.78 (quin, J = 7.1 Hz, 2H), 1.73 (quin, J = 7.1 Hz, 2H), 1.48 (quin, J = 7.1 Hz, 2H), 1.44 (quin, J = 7.1 Hz, 2H), 1.42−1.28 (m, 8H), 0.89 (t, J = 7.1 Hz, 3H), 0.61 (t, J = 7.1 Hz, 3H). ^{13}C NMR (CD_3CN): δ 168.7, 161.3, 157.6, 149.4, 145.3, 131.3, 127.7, 123.6, 118 (covered by solvent peak; see the Supporting Information), 106.4, 100.2, 68.6, 68.2, 62.2, 46.8, 31.4, 31.3, 29.0, 28.9, 25.6, 25.5, 22.5, 22.3, 13.4, 13.4. ESI-HRMS: calcd for $[M + H]^+$ $C_{28}H_{40}BN_2O_6$ 511.2974, found 511.2985.

*Diisobutyl 6,6′-Dichloro-2,2′-bipyridine-4′,4′-dicarboxylate (**6**).* *m*-Chloroperbenzoic acid (5.0 g, 29 mmol) was added to a solution of diisobutyl 4,4′-bipyridinedicarboxylate[25] (2.0 g, 5.6 mmol) in $CHCl_3$ (50 mL), and the mixture was stirred for 3 days at room temperature. The solvent was evaporated under reduced pressure and water was added. The aqueous mixture was extracted with CH_2Cl_2 (3 × 50 mL). The dried organic layers were evaporated to dryness, affording diisobutyl-4,4′-bipyridinedicarboxylate dioxide as a yellow solid (2.0 g, 5.2 mmol, 92%). ^1H NMR ($CDCl_3$): δ 8.34 (d, 6.8 Hz, 2H), 8.14 (d, J = 2.3 Hz, 2H), 7.98 (dd, J = 2.5, 7.0 Hz, 2H), 4.13 (d, J = 6.7 Hz, 4H), 2.07 (sep, J = 7.6 Hz, 2H), 1.00 (d, J = 6.7 Hz, 12H). A solution of diisobutyl-4,4′-bipyridinedicarboxylate dioxide (1.3 g, 3.5 mmol) in $POCl_3$ (16 mL) was refluxed for 7 h. At room temperature, a saturated aqueous solution of $NaHCO_3$ was carefully added. The formed brown precipitate was collected by filtration and purified by flash chromatography (CH_2Cl_2/ethyl acetate 8:2) affording the product **6** (1.1 g, 2.6 mmol, 77%) as a white powder. Mp: 109−114 °C. ^1H NMR ($CDCl_3$): δ 8.84 (s, 2H), 7.92 (s, 2H), 4.19 (d, J = 6.7 Hz, 4H), 2.14 (sep, J = 7.6 Hz, 2H), 1.04 (d, 6.7 Hz, 12H). ^{13}C NMR ($CDCl_3$): δ 163.8 (C, 2C), 155.5 (C, 2C), 151.9 (C, 2C), 141.8 (C, 2C), 124.7 (CH, 2C), 119.5 (CH, 2C), 72.2 (CH_2, 2C), 27.8 (CH, 2C), 19.1 (CH_3, 4C). ESI-HRMS: calcd for $[M + Na]^+$ $C_{20}H_{22}Cl_2N_2NaO_4$ 447.0849, found 447.0856.

*4′,4″-Dicarboxylic-2,2′:6′,2″:6″,2‴-quaterpyridine Diisobutyl Ester (**1a**).* Pd_2dba_3 (143 mg, 0.15 mmol) and 2-dicyclohexylphosphino-2′,4′,6′-triisopropylbiphenyl (XPhos) (298 mg, 0.62 mmol) were added to a Schlenk flask under ambient atmosphere. DMF (4 mL) and isopropyl alcohol (IPA) (10 mL) were added under an argon atmosphere. The mixture was stirred under argon at 100 °C for 1 h and then injected by syringe at 50 °C to a Schlenk flask previously charged with **6** (2.0 g, 4.7 mmol), **1b** (3.6 g, 15 mmol), $Cu(OAc)_2$ (946 mg, 5.2 mmol), and K_2CO_3 (7.2 g, 52 mmol) under an argon atmosphere. The mixture was stirred under argon at 100 °C for 15 h. An aqueous solution of NaOH 1 M (400 mL) was added at room temperature and the mixture extracted with CH_2Cl_2 (3 × 50 mL). The solvent was evaporated from the collected and dried organic layers leaving a residue which was taken up with CH_2Cl_2 (1 mL) and cyclohexane (50 mL). The product was isolated as a brown precipitate (786 mg, 1.54 mmol, 33%). Mp: 170−175 °C. ^1H NMR ($CDCl_3$): δ 9.20 (d, J = 1.5 Hz, 2H), 9.04 (d, J = 1.5 Hz, 2H), 8.76 (d, J = 4.0 Hz, 2H), 8.70 (s, J = 8.0 Hz, 2H), 7.91 (dd, J = 2.0, 9.5 Hz, 2H), 7.39 (dd, J = 5. 6, 1.5 Hz, 2H), 4.25 (d, J = 6.5 Hz, 4H), 2.21 (sep, J = 6.5 Hz, 2H), 1.10 (d, 6.7 Hz, 12H). ^{13}C NMR ($CDCl_3$): δ 165.5 (C, 2C), 156.8 (C, 2C), 155.8 (C, 2C), 155.3 (C, 2C), 149.3 (CH, 2C), 140.1 (C, 2C), 137.0 (CH, 2C), 124.2 (CH, 2C), 121.4 (CH, 2C), 120.6 (CH, 2C), 120.5 (CH, 2C), 71.8 (CH_2, 2C), 27.9 (CH, 2C), 19.2 (CH_3, 4C). ESI-HRMS: calcd for $[M + Na]^+$ $C_{30}H_{30}N_4NaO_4$ 533.2159, found 533.2156. Anal. Calcd for $C_{30}H_{30}N_4O_4 \cdot {}^1/_5$cyclohexane: C, 71.05; H, 6.19; N, 10.62. Found: C, 70.62; H, 5.92; N, 10.26.

*6,6‴-Dimethyl-4′,4″-dicarboxylic-2,2′:6′,2″:6″,2‴-quaterpyridine Diisobutyl Ester (**2a**).* A procedure similar to the synthesis of **1a** was applied starting from Pd_2dba_3 (28 mg, 0.031 mmol), XPhos (54 mg, 0.11 mmol), DMF (8 mL), IPA (2 mL), **6** (400 mg, 0.94 mmol), **2b** (934 mg, 3.8 mmol), $Cu(OAc)_2$ (188 mg, 1.0 mmol), and K_2CO_3 (1.4 g, 10 mmol). After the reaction mixture was stirred for 15 h at 100 °C under argon, an aqueous solution of NaOH 1 M (90 mL) was added affording the product as a brown precipitate (105 mg, 0.19 mmol, 21%). Mp: 173−178 °C (cyclohexane). ^1H NMR ($CDCl_3$): δ 9.18 (d, J = 1.2 Hz, 2H), 9.05 (d, J = 1.2 Hz, 2H), 8.48 (d, J = 7.8 Hz, 2H), 7.78 (t, J = 8.0 Hz, 2H), 7.25 (d, 7.7 Hz, 2H), 4.26 (d, J = 6.5 Hz, 4H), 2.68 (s, 6H), 2.20 (sep, J = 7.6 Hz, 2H), 1.11 (d, J = 6.7 Hz, 12H). ^{13}C NMR ($CDCl_3$): δ 165.6 (C, 2C), 158.1 (C, 2C), 157.1 (C, 2C), 155.8 (C, 2C), 154.7 (C, 2C), 140.0 (C, 2C), 137.1 (CH, 2C), 123.8 (CH, 2C), 120.6 (CH, 2C), 120.3 (CH, 2C), 118.4 (CH, 2C), 71.7 (CH_2, 2C), 27.9 (CH, 2C), 24.6 (CH_3, 2C), 19.2 (CH_3, 4C). ESI-HRMS: calcd for $[M + Na]^+$ $C_{32}H_{34}N_4NaO_4$ 561.2472, found 561.2469. Anal. Calcd for $C_{32}H_{34}N_4O_4 \cdot {}^1/_5$cyclohexane: C, 71.79; H, 6.61; N, 10.09. Found: C, 71.95; H, 6.12; N, 9.75.

*6,6‴-Dimethoxy-4′,4″-dicarboxylic-2,2′:6′,2″:6″,2‴-quaterpyridine Diisobutyl Ester (**3a**).* A procedure similar to the synthesis of **1a** was applied starting from Pd_2dba_3 (13 mg, 0.014 mmol), XPhos (27 mg, 0.050 mmol), DMF (4 mL), IPA (1 mL), **6** (200 mg, 0.47 mmol), **3b** (373 mg, 1.41 mmol), $Cu(OAc)_2$ (175 mg, 0.47 mmol), and K_2CO_3 (389 mg, 2.8 mmol). After the reaction mixture was stirred for 15 h at 100 °C under an argon atmosphere, H_2O (20 mL) was added at room temperature and a black solid was collected by filtration and taken up with CH_2Cl_2 (1 mL). Petroleum ether (50 mL) was added to the resulting solution yielding the product as a brown solid (91 mg, 0.16 mmol, 34%). Mp: 202−207 °C. ^1H NMR ($CDCl_3$): δ 9.16 (d, J = 1.2 Hz, 2H), 9.02 (d, J = 1.2 Hz, 2H), 8.30 (d, J = 7.3 Hz, 2H), 7.78 (t, J = 7.7 Hz, 2H), 6.85 (d, J = 8.2 Hz, 2H), 4.25 (d, J = 6.5 Hz, 4H), 4.11 (s, 6H), 2.20 (sep, J = 7.6 Hz, 2H), 1.13 (d, 6.7 Hz, 12H). ^{13}C

dx.doi.org/10.1021/jo301226z | J. Org. Chem. 2012, 77, 7945−7956

NMR ($CDCl_3$): δ 165.6 (C, 2C), 163.4 (C, 2C), 156.6 (C, 2C), 155.7 (C, 2C), 152.5 (C, 2C), 139.9 (C, 2C), 139.4 (CH, 2C), 120.5 (CH, 2C), 120.3 (CH, 2C), 114.1 (CH, 2C), 111.8 (CH, 2C), 71.6 (CH_2, 2C), 53.3 (CH_3, 2C), 28.0 (CH, 2C), 19.1 (CH_3, 4C). Anal. Calcd for $C_{32}H_{34}N_4O_6 \cdot {}^1/_{10}$cyclohexane: C, 67.62; H, 6.13; N, 9.68. Found: C, 67.22; H, 6.47; N, 9.47.

*4,4‴-Bis(5-hexylthien-2-yl)-4′,4″-dicarboxylic-2,2′:6′,2″:6″,2‴-quaterpyridine Diisobutyl Ester (**4a**).* A procedure similar to the synthesis of **1a** was applied starting from Pd_2dba_3 (4.0 mg, 0.0041 mmol), XPhos (9.0 mg, 0.019 mmol), DMF (4 mL), IPA (1 mL), **6** (54 mg, 0.12 mmol), **4b** (150 mg, 0.37 mmol), $Cu(OAc)_2$, and K_2CO_3 (104 mg, 0.75 mmol). After the reaction mixture was stirred for 15 h at 100 °C under argon, H_2O (20 mL) was added at room temperature and a brown solid was obtained as a precipitate. The solid was dissolved in CH_2Cl_2 (1 mL), and then petroleum ether (50 mL) was added giving a brown precipitate (40 mg). The NMR analysis showed the presence of aliphatic impurities. Then the sample was dissolved in CH_3CN (2 mL), and NBu_4OH 1 M (0.3 mL) was added. After the mixture was stirred at room temperature for 2 h, CH_3CN was evaporated from the mixture and H_2O (2 mL) was added. After (pH = 7) the mixture was neutralized with HNO_3 0.1 M and left at −4 °C for 15 h, a green solid was obtained which was collected by filtration and dissolved in *i*-BuOH (5 mL). Concentrated sulfuric acid (3 drops) was added and the mixture refluxed for 6 h. *i*-BuOH was evaporated under reduced pressure, H_2O (3 mL) was added and the pH of the solution adjusted to 7 with a saturated aqueous solution of $NaHCO_3$ affording the pure product as a brown precipitate (40 mg, 0.047 mmol, 39%). Mp: 166−171 °C. ^{1}H NMR ($CDCl_3$): δ 9.23 (s, 2H), 9.09 (s, 2H), 8.83 (s, 2H), 8.72 (d, *J* = 4.9 Hz, 2H), 7.54 (d, *J* = 2.8 Hz, 2H), 7.52 (d, *J* = 4.8 Hz, 2H), 6.86 (d, *J* = 2.8 Hz, 2H), 4.26 (d, *J* = 6.5 Hz, 4H), 2.89 (t, *J* = 7.6 Hz, 4H), 2.24 (sep, *J* = 6.5 Hz, 2H), 1.74 (quin, *J* = 7.0 Hz, 4H), 1.42 (quin, *J* = 7.1 Hz, 4H), 1.39−1.32 (m, 8H) 1.09 (d, *J* = 6.7 Hz, 12H), 0.90 (t, *J* = 7.0 Hz, 6H). ^{13}C NMR ($CDCl_3$): δ 165.5, 156.0, 150.0, 148.8, 143.0, 140.2, 140.1, 138.6, 125.7, 125.7, 121.2, 120.8, 120.2, 117.1, 117.1, 72.0, 31.7. 31.7, 30.5, 28.9, 28.0, 22.7, 19.5, 14.2. ESI-HRMS: calcd for $[M + Na]^+$ $C_{50}H_{58}N_4NaO_4S_2$ 865.3792, found 865.3789. Anal. Calcd for $C_{50}H_{58}N_4O_4S_2 \cdot {}^1/_{10}$cyclohexane: C, 71.37; H, 7.01; N, 6.58. Found: C, 71.75; H, 7.04; N, 7.04.

*4,4‴-Bis(2,4-dihexyloxyphenyl)-4′,4″-dicarboxylic-2,2′:6′,2″:6″,2‴-quaterpyridine Diisobutyl Ester (**5a**).* A procedure similar to the synthesis of **1a** was applied starting from Pd_2dba_3 (5.0 mg, 0.0060 mmol), XPhos (13 mg, 0.027 mmol), DMF (4 mL), IPA (1 mL), **6** (25 mg, 0.06 mmol), **5b** (91 mg, 0.18 mmol), $Cu(OAc)_2$ (12 mg, 0.066 mmol), and K_2CO_3 (25 mg, 0.18 mmol). After the mixture was stirred for 15 h at 100 °C under Ar, H_2O (20 mL) was added at room temperature. After the mixture was extracted with CH_2Cl_2 (3 × 20 mL), the solvent was evaporated from the collected organic layers, leaving a oily residue which was submitted to flash chromatography (CH_2Cl_2/ethyl acetate 95:5). The pure product was obtained as a white solid (25 mg, 0.023 mmol, 39%). Mp: 112−117 °C. ^{1}H NMR ($CDCl_3$): δ 9.16 (s, 2H), 9.08 (s broad, 2H), 8.85 (s, 2H), 8.72 (d, *J* = 5.0 Hz, 2H), 7.59 (s broad, 2H), 7.43 (d, *J* = 7.0 Hz, 2H), 6.65−6.60 (m, 4H), 4.19 (d, *J* = 6.7 Hz, 4H), 4.08−4.00 (m, 8H), 2.12 (sep, *J* = 7.6 Hz, 2H), 1.82 (quin, *J* = 7.1 Hz, 4H), 1.72 (quin, *J* = 7.1 Hz, 4H), 1.55−1.45 (m, 6H), 1.42−1.30 (m, 14H), 1.15−1.05 (m, 10H), 1.00 (d, *J* = 6.7 Hz, 12H), 0.93 (t, *J* = 6.9 Hz, 6H), 0.70 (t, *J* = 6.9 Hz, 6H). ^{13}C NMR ($CDCl_3$): δ 165.6, 161.2, 157.6, 157.4, 156.0, 155.1, 148.9, 147.6, 140.1, 131.1, 125.0, 122.0, 120.9, 120.8, 120.4, 105.8, 100.4, 71.8, 68.7, 68.3, 31.7, 31.5, 29.4, 29.2, 28.0, 25.9, 25.8, 22.7, 22.5, 19.3, 14.2, 14.0. ESI-HRMS: calcd for $[M + Na]^+$ $C_{66}H_{86}N_4NaO_8$ 1085.6343, found 1085.6328. Anal. Calcd for $C_{66}H_{86}N_4O_8$: C, 74.54; H, 8.15; N, 5.27. Found: C, 74.93; H, 8.61; N, 5.51.

*trans-Dithiocyanato [Ru(4′,4″-dicarboxylic-2,2′:6′,2″:6″,2‴-quaterpyridine diisobutyl ester)] (**1e**).* A solution of dichloro(*p*-cymene)-ruthenium(II) dimer (60 mg, 0.098 mmol) and **1a** (100 mg, 0.20 mmol) in DMF (15 mL) was shielded from light and stirred for 2 h at 100 °C and for 4 h at 140 °C under an argon atmosphere. After magnetic stirring at room temperature for 15 h, NH_4NCS (605 mg, 8.0 mmol) was added and the mixture was stirred for 4 h at 140 °C and for 15 h at room temperature. H_2O (10 mL) was added to the mixture and the dark precipitate isolated and purified by flash chromatography (CH_2Cl_2/acetone 97:3) to afford the product as a red solid (60 mg, 0.082 mmol, 42%). ^{1}H NMR (DMSO-d_6): δ 9.74 (d, *J* = 5.1 Hz, 2H), 9.17 (d, *J* = 1.1 Hz, 2H), 9.10 (d, *J* = 1.1 Hz, 2H), 8.98 (d, *J* = 8.1 Hz, 2H), 8.41 (td, *J* = 1.5, 7.9 Hz, 2H), 8.05 (t, *J* = 6.4 Hz, 2H), 4.28 (d, *J* = 6.7 Hz, 4H), 2.18 (sep, *J* = 6.7 Hz, 2H), 1.09 (d, *J* = 6.7 Hz, 12H). ^{13}C NMR (CD_2Cl_2): δ 163.8, 160.3, 159.6, 158.0, 153.6, 139.4, 134.4, 131.9, 128.5, 123.4, 121.9, 121.2, 72.6, 28.1, 19.0. ESI-HRMS: calcd for $[M + Na]^+$ $C_{32}H_{30}N_6NaO_4RuS_2$ 751.0706, found 751.0711.

*trans-Dithiocyanato [Ru(4′,4″-dicarboxylic-2,2′:6′,2″:6″,2‴-quaterpyridine)] (**1d**).* NBu_4OH 1 M (0.5 mL) was added to a solution of **1e** (60 mg, 0.082 mmol) in CH_3CN (5 mL). After the mixture was stirred at room temperature for 15 h, CH_3CN was evaporated, H_2O (5 mL) was added, and pH was adjusted to 3−3.5 by adding HNO_3 0.1 M. The mixture was allowed to rest at −4 °C for 15 h affording the pure product as a red precipitate (20 mg, 0.032 mmol, 40%). ^{1}H NMR (MeOD): δ 9.57 (d, *J* = 4.4 Hz, 2H), 8.90 (s, 2H), 8.83 (s, 2H), 8.57 (d, *J* = 8.1 Hz, 2H), 8.23 (t, *J* = 7.3 Hz, 2H), 7.91 (t, *J* = 4.9 Hz, 2H).[34] ESI-HRMS: calcd for $[M - H]^-$ $C_{24}H_{13}N_6O_4RuS_2$ 614.9489, found 614.9509.

Electrochemical Characterization. The qpys **1a**−**5a** were dissolved (10^{-4} M) in a 0.1 M solution of tetrabutylammonium perchlorate ($TBAClO_4$) in anhydrous CH_2Cl_2. The complexes **1d** and **1e** (10^{-4} M) were characterized in tetrabutylammonium hexafluorophosphate ($TBAPF_6$) in anhydrous DMF. DPV and CV were carried out at a scan rate of 20 and 50 mV/s, respectively, with a potentiostat in a three-electrode electrochemical cell. All the measurements were carried out in a glovebox filled with argon ($[O_2]$<1 ppm). The working, counter, and pseudoreference electrodes were a well-polished Au pin, a Pt flag, and a Ag/AgCl wire, respectively. The Ag/AgCl pseudoreference electrode was externally calibrated by adding ferrocene (10^{-3} M) to the electrolyte. For the spectroelectrochemical analysis a thin layer electrochemical cell was used equipped with a Au gauze working electrode. Sprectra were collected at different applied potential in the wavelength range from 260 to 800 nm.

Computational Investigation. All the calculations have been performed by the GAUSSIAN 03 program package.[35] We optimized the molecular structures of **1a**−**5a** and **1d** in vacuum using the B3LYP exchange−correlation functional[36] and a 3-21G* basis set.[37] TDDFT calculations of the lowest singlet−singlet excitations were performed for **1a**−**5a** compounds using B3LYP and MPW1K[38] xc functional with a 6-31G* basis set,[39] while for the complex **1d** we used B3LYP xc functional and a DGDZVP basis set.[40] Solvent (CH_2Cl_2 and DMF) effects were included by the PCM nonequilibrium version[41] as implemented in GAUSSIAN 03.

■ ASSOCIATED CONTENT

Supporting Information

Tauc plots of qpy **1a**−**5a** and complex **1d**; excitation spectra of qpy **1a**−**5a**; UV−vis spectra of deprotonated **1d** in DMF and MeOH; CV current/potential profiles of qpy **1a**−**3a** and **5a**; CV current/potential profiles for complexes **1d** and **1e**; spectroelectrochemistry of complex **1d**; comparison between computed and experimental UV−vis spectra of qpy **1a**−**5a** and complex **1d**; ^{1}H and ^{13}C NMR spectra of **4b**, **5c**, **5b**, **6**, **1a**−**5a**, and **1e** and ^{1}H NMR spectrum of **1d**; energies of the lowest unoccupied and highest occupied Kohn−Sham orbitals of qpy **1a**−**5a** and **1d**; comparison between computed excitation energies and oscillator strengths for the optical transitions of qpy **1a**−**5a** and complex **1d**; computed Cartesian coordinates and total energy of compounds **1a**−**5a** and **1d**. This material is available free of charge via the Internet at http://pubs.acs.org/.

dx.doi.org/10.1021/jo301226z | J. Org. Chem. 2012, 77, 7945−7956

AUTHOR INFORMATION

Corresponding Author

*E-mail: alessandro.abbotto@unimib.it; filippo@thch.unipg.it.

Notes

The authors declare no competing financial interest.

ACKNOWLEDGMENTS

We thank FP7-ENERGY-2010 project 261920 "ESCORT" for financial support.

REFERENCES

(1) (a) Dalton, L. R.; Sullivan, P. A.; Bale, D. H. *Chem. Rev.* **2010**, *110*, 25−55. (b) Luo, J.; Zhou, X.-H.; Jen, A. K.-Y. *J. Mater. Chem.* **2009**, *19*, 7410−7424.

(2) He, G. S.; Tan, L.-S.; Zheng, Q.; Prasad, P. N. *Chem. Rev.* **2008**, *108*, 1245−1330.

(3) *Organic Photovoltaics*; Brabec, C. J., Dyakanov, V., Parisi, J., Sariciftci, N. S., Eds.; Springer: Berlin, 2003.

(4) (a) *Highly Efficient OLEDs with Phosphorescent Materials*; Yersin, H., Ed.; Wiley-VCH: Berlin, 2007. (b) Wong, W.-Y.; Ho, C.-L. *Coord. Chem. Rev.* **2009**, *253*, 1709−1758. (c) Evans, R. C.; Douglas, P.; Winscom, C. J. *Coord. Chem. Rev.* **2006**, *250*, 2093−2126. (d) Chou, P.-T.; Chi, Y. *Chem.—Eur. J.* **2007**, *13*, 380−395.

(5) (a) O'Regan, B.; Graetzel, M. *Nature* **1991**, *353*, 737−740. (b) Graetzel, M. *Nature* **2001**, *414*, 338−344.

(6) *Dye-Sensitized Solar Cells*; Kalyanasundaram, K., Ed.; EPFL/CRC Press: Lausanne, 2010.

(7) Reviews: (a) Elliott, C. M. *Nature Chem.* **2011**, *3*, 188−189. (b) Nazeeruddin, M. K.; Baranoff, E.; Grätzel, M. *Solar Energy* **2011**, *85*, 1172−1178. (c) Hagfeldt, A.; Boschloo, G.; Sun, L.; Kloo, L.; Pettersson, H. *Chem. Rev.* **2010**, *110*, 6595−6663. (d) Grätzel, M. *Acc. Chem. Res.* **2009**, *42*, 1788−1798.

(8) Nazeeruddin, M. K.; DeAngelis, F.; Fantacci, S.; Selloni, A.; Viscardi, G.; Liska, P.; Ito, S.; Takeru, B.; Grätzel, M. *J. Am. Chem. Soc.* **2005**, *127*, 16835−16847.

(9) Review: Abbotto, A.; Manfredi, N. *Dalton Trans.* **2011**, *40*, 12421−12438.

(10) (a) Abbotto, A.; Barolo, C.; Bellotto, L.; Angelis, F. D.; Gratzel, M.; Manfredi, N.; Marinzi, C.; Fantacci, S.; Yum, J.-H.; Nazeeruddin, M. K. *Chem. Commun.* **2008**, *42*, 5318−5320. (b) Abbotto, A.; Bellotto, L.; Angelis, F. D.; Manfredi, N.; Marinzi, C. *Eur. J. Org. Chem.* **2008**, *2008*, 5047−5054.

(11) Coluccini, C.; Manfredi, N.; Calderon, E. H.; Salamone, M. M.; Ruffo, R.; Roberto, D.; Lobello, M. G.; De Angelis, F.; Abbotto, A. *Eur. J. Org. Chem.* **2011**, *2011*, 5587−5598.

(12) Pechy, P.; Renouard, T.; Zakeeruddin, S. M.; Humphry-Baker, R.; Comte, P.; Liska, P.; Cevey, L.; Costa, E.; Shklover, V.; Spiccia, L.; Deacon, G. B.; Bignozzi, C. A.; Grätzel, M. *J. Am. Chem. Soc.* **2001**, *123*, 1613−1624.

(13) (a) Renouard, T.; Gratzel, M. *Tetrahedron* **2001**, *57*, 8145−8150. (b) Renouard, T.; Fallahpour, R.-A.; Nazeeruddin, M. K.; Humphry-Baker, R.; Gorelsky, S. I.; Lever, A. B. P.; Grätzel, M. *Inorg. Chem.* **2002**, *41*, 367−378. (c) Barolo, C.; Nazeeruddin, M. K.; Fantacci, S.; DiCenso, D.; Comte, P.; Liska, P.; Viscardi, G.; Quagliotto, P.; DeAngelis, F.; Ito, S.; Grätzel, M. *Inorg. Chem.* **2006**, *45*, 4642−4653.

(14) Abbotto, A.; Sauvage, F.; Barolo, C.; De Angelis, F.; Fantacci, S.; Grätzel, M.; Manfredi, N.; Marinzi, C.; Nazeeruddin, M. K. *Dalton Trans.* **2011**, *40*, 234−242.

(15) Constable, E. C.; Elder, S. M.; Hannon, M. J.; Martin, A.; Raithby, P. R.; Tocher, D. A. *J. Chem. Soc., Dalton Trans.* **1996**, *12*, 2423−2433.

(16) (a) Yeung, H.-L.; Wong, W.-Y.; Wong, C.-Y.; Kwong, H.-L. *Inorg. Chem.* **2009**, *48*, 4108−4117. (b) Yeung, H.-L.; Sham, K.-C.; Wong, W.-Y.; Wong, C.-Y.; Kwong, H.-L. *Eur. J. Inorg. Chem.* **2011**, *2011*, 5112−5124.

(17) Suzuki, A. Cross-coupling Reactions of Organoboron Compounds with Organic Halides. In *Metal-catalyzed Cross-coupling Reactions*; Diederich, F., Stang, P. J., Eds.; Wiley-VCH: Weinheim, 1998; Chapter 2.

(18) (a) Tsao, H. N.; Yi, C.; Moehl, T.; Yum, J.-H.; Zakeeruddin, S. M.; Nazeeruddin, M. K.; Grätzel, M. *ChemSusChem* **2011**, *4*, 591−594. (b) Dualeh, A.; De Angelis, F.; Fantacci, S.; Moehl, T.; Yi, C.; Kessler, F.; Baranoff, E.; Nazeeruddin, M. K.; Grätzel, M. *J. Phys. Chem. C* **2011**, *116*, 1572−1578.

(19) Yum, J.-H.; Baranoff, E.; Kessler, F.; Moehl, T.; Ahmad, S.; Bessho, T.; Marchioro, A.; Ghadiri, E.; Moser, J.-E.; Yi, C.; Nazeeruddin, M. K.; Grätzel, M. *Nature Commun.* **2012**, *3*, 631.

(20) Yella, A.; Lee, H. -W.; Tsao, H. N.; Yi, C.; Chandiran, A. K.; Nazeeruddin, M. K.; Diau, E. W.-G.; Yeh, C.-Y.; Zakeeruddin, S. M.; Grätzel, M. *Science* **2011**, *334*, 629−634.

(21) Knapp, D. M.; Gillis, E. P.; Burke, M. D. *J. Am. Chem. Soc.* **2009**, *131*, 6961−6963.

(22) Dick, G. R.; Woerly, E. M.; Burke, M. D. *Angew. Chem., Int. Ed.* **2012**, *51*, 2667−2672.

(23) Dick, G. R.; Knapp, D. M.; Gillis, E. P.; Burke, M. D. *Org. Lett.* **2010**, *12*, 2314−2317.

(24) Coluccini, C.; Manfredi, N.; Calderon, E. H.; Salamone, M. M.; Ruffo, R.; Roberto, D.; Lobello, M. G.; De Angelis, F.; Abbotto, A. *Eur. J. Org. Chem.* **2011**, *2011*, 5587−5598.

(25) Rawling, T.; Buchholz, F.; McDonagh, A. M. *Aust. J. Chem.* **2008**, *61*, 405−408.

(26) Tauc, J. *Mater. Res. Bull.* **1968**, *3*, 37−46.

(27) Pechy, P.; Renouard, T.; Zakeeruddin, S. M.; Humphry-Baker, R.; Comte, P.; Liska, P.; Cevey, L.; Costa, E.; Shklover, V.; Spiccia, L.; Deacon, G. B.; Bignozzi, C. A.; Grätzel, M. *J. Am. Chem. Soc.* **2001**, *123*, 1613−1624.

(28) Nazeeruddin, M. K.; Humphry-Baker, R.; Liska, P.; Grätzel, M. *J. Phys. Chem. B* **2003**, *107*, 8981−8987.

(29) Wolfbauer, G.; Bond, A. M.; Deacon, G. B.; MacFarlane, D. R.; Spiccia, L. *J. Am. Chem. Soc.* **1999**, *122*, 130−142.

(30) Kümper, S.; Paretzki, A.; Fiedler, J.; Záliš, S.; Kaim, W. *Inorg. Chem.* **2012**, *51*, 2097−2104.

(31) (a) Falciola, L.; Gennaro, A.; Isse, A. A.; Mussini, P. R.; Rossi, M. *J. Electroanal. Chem.* **2006**, *593*, 47−56. (b) Bockris, J. O. M.; Khan, S. U. M. *Surface Electrochemistry − A Molecular Level Approach*; Kluwer Academic/Plenum Publishers: New York; 1993.

(32) Pastore, M.; Mosconi, E.; De Angelis, F.; Grätzel, M. *J. Chem. Phys. C* **2010**, *114*, 7205−7212.

(33) Investigation of DSC devices with this and other qpy-based Ru(II) photosensitizers is currently in progress and will be reported in due course.

(34) The ^{13}C NMR spectrum could not be recorded because of the low solubility in common organic solvents.

(35) Frisch, M. J.; Trucks, G. W.; Schlegel, H. B.; Scuseria, G. E.; Robb, M. A.; Cheeseman, J. R.; Montgomery, J. A., Jr.; Vreven, T.; Kudin, K. N.; Burant, J. C.; Millam, J. M.; Iyengar, S. S.; Tomasi, J.; Barone, V.; Mennucci, B.; Cossi, M.; Scalmani, G.; Rega, N.; Petersson, G. A.; Nakatsuji, H.; Hada, M.; Ehara, M.; Toyota, K.; Fukuda, R.; Hasegawa, J.; Ishida, M.; Nakajima, T.; Honda, Y.; Kitao, O.; Nakai, H.; Klene, M.; Li, X.; Knox, J. E.; Hratchian, H. P.; Cross, J. B.; Bakken, V.; Adamo, C.; Jaramillo, J.; Gomperts, R.; Stratmann, R. E.; Yazyev, O.; Austin, A. J.; Cammi, R.; Pomelli, C.; Ochterski, J. W.; Ayala, P. Y.; Morokuma, K.; Voth, G. A.; Salvador, P.; Dannenberg, J. J.; Zakrzewski, V. G.; Dapprich, S.; Daniels, A. D.; Strain, M. C.; Farkas, O.; Malick, D. K.; Rabuck, A. D.; Raghavachari, K.; Foresman, J. B.; Ortiz, J. V.; Cui, Q.; Baboul, A. G.; Clifford, S.; Cioslowski, J.; Stefanov, B. B.; Liu, G.; Liashenko, A.; Piskorz, P.; Komaromi, I.; Martin, R. L.; Fox, D. J.; Keith, T.; Al-Laham, M. A.; Peng, C. Y.; Nanayakkara, A.; Challacombe, M.; Gill, P. M. W.; Johnson, B.; Chen, W.; Wong, M. W.; Gonzalez, C.; Pople, J. A. Gaussian 03, revision C.02; Gaussian, Inc.: Wallingford, CT, 2004.

(36) Becke, A. D. *J. Chem. Phys.* **1993**, *98*, 5648−5652.

(37) Binkley, J. S.; Pople, J. A.; Hehre, W. J. *J. Am .Chem. Soc.* **1980**, *102*, 939−947.

(38) Lynch, B. J.; Fast, P. L.; Harris, M.; Truhlar, D. G. *J. Phys. Chem. A* **2000**, *104*, 4811−4815.
(39) Ditchfield, R.; Hehre, W. J.; Pople, J. A. *J. Chem. Phys.* **1971**, *54*, 724−728.
(40) Godbout, N.; Salahub, D. R.; Andzelm, J. *Erich, W. Can. J. Chem.* **1992**, *70*, 560−571.
(41) Cossi, M.; Barone, V. *J. Chem. Phys.* **2001**, *115*, 4708−4717.